Bull Volcanol (2016) 78: 9
DOI 10.1007/s00445-016-1007-6

RESEARCH ARTICLE

A debris avalanche at Süphan stratovolcano (Turkey) and implications for hazard evaluation

Yavuz Özdemir[1] · **İsmail Akkaya**[2] · **Vural Oyan**[3] · **Karim Kelfoun**[4]

Received: 27 May 2015 / Accepted: 28 January 2016 / Published online: 9 February 2016

Abstract The Quaternary Süphan debris avalanche deposit is located in Eastern Anatolia, Turkey. The avalanche formed by the sector collapse of a major stratovolcano towards the north, possibly during a single catastrophic event. The deposit has an estimated volume of 4 km^3 and ran out over 25 km to cover an area of approximately 200 km^2. Products of the collapse are overlain by younger eruptive units from the Süphan volcano. We have tested the numerical code *VolcFlow* to first reproduce the emplacement of the Quaternary Süphan debris avalanche and then to develop a hazard assessment for potential future sector collapses and subsequent emplacement of debris avalanches and associated tsunami. The numerical model captures the main features of the propagation process, including travel distance, lateral spread, and run up. The best fit obtained for the existing flow has a constant retarding stress of 50 kPa and a collapse scar volume of 4 km^3. Analysis of potential future collapse scenarios reveals that northern sector debris avalanches (up to 6 km^3) could affect several towns. In the case of a sector collapse towards the south, a tsunami will reach the city of Van and several of the biggest towns on the southern shoreline of Lake Van. Cities most affected by the larger amplitude waves would be Van, Edremit, Gevaş, Tatvan, and, to a lesser extent, Erciş, with wave amplitudes (first waves after the onset of the collapse) between 8 and 10 m.

Keywords Süphan stratovolcano · Eastern anatolia · Debris avalanche · Tsunami · Volcflow

Editorial responsibility: J. Taddeucci

✉ Yavuz Özdemir
yozdemir@yyu.edu.tr

[1] Department of Geological Engineering, Yuzuncu Yıl University, Van, Turkey

[2] Department of Geophysical Engineering, Yuzuncu Yıl University, Van, Turkey

[3] Department of Mining Engineering, Yuzuncu Yıl University, Van, Turkey

[4] Laboratoire Magmas et Volcans, Université Blaise Pascal, Clermont-Ferrand, France

Introduction

Volcanic debris avalanches result from the catastrophic collapse of flanks of volcanic edifices (Ui 1983; Siebert 1984). They are common events in the history of many volcanoes (Siebert et al. 1987). In just a few minutes, a debris avalanche can fill and change the surrounding landscape and cover extensive areas. Debris avalanche deposits extending beyond the flanks of volcanoes have been detected at more than 350 edifices around the world (Siebert 2002), although many more must exist. Volcanic debris avalanches are one of the most destructive hazards for inhabited areas around volcanoes, directly or through secondary events, such as tsunamis (Keating and McGuire 2000; Sosio et al. 2011), lahars (Scott et al. 2005; Sosio et al. 2011), or magmatic eruptions (e.g., Mc Guire 1996; Sosio et al. 2011; Borselli et al. 2011). Debris avalanches have caused approximately 20,000 casualties in the last 400 years (Siebert 1984).

The volumes of volcanic debris avalanche deposits vary from 0.1 to 45 km^3 and run out distances can exceed 100 km (Stoopes and Sheridan 1992). Such deposits are characterized by two depositional facies, “block” and “matrix” (Ui 1989; Ui et al., 2000). The processes that form the debris avalanches are variable, but three typical styles of debris avalanches have been proposed based on: Bezymianny, Bandai, and Unzen (Sigurdsson et al. 2000). Bezymianny debris

avalanches are associated with magmatic eruptions, as in the case of Mount St. Helens in 1980 (e.g., Voight et al. 1981, 1983; Glicken 1986). Magmatic eruptions that shortly follow edifice collapse such as the Mount St Helens eruption can produce extensive pyroclastic density currents and fallout (Siebert 1984; Siebert et al. 1987). Bandai-type avalanches are associated with phreatic or hydrothermal eruptions, as in the case of Bandai, Japan, in 1888. No juvenile material is included within this type of deposit. An Unzen-type avalanche is not directly related to volcanic activity, but is instead triggered by an earthquake (Siebert et al. 1987). A new type of edifice collapse has been recently recognized in Casita-type events that result from extreme rainfall onto a previously weakened and hydrothermally altered edifice (van Wyk de Vries et al. 2000; Scott et al. 2001; Kerle et al., 2001, 2003a, b; Devoli et al. 2009). Edifice collapse can occur on a variety of volcanic structures from stratovolcanoes to dome complexes. In an active volcanic area, the triggering cause of edifice collapse could be magmatic, phreatomagmatic, or seismic, and the first two causes are normally associated with dome-growth deformation and explosive eruptions (Glicken 1996; Mc Guire 1996). The instability of a volcanic edifice is promoted by many factors directly related to volcanic activity, as well as exogenous forcing processes such as tectonic seismicity, extreme rainfall, and hydrothermal alteration.

The most active and voluminous Quaternary volcanoes of Turkey are situated in eastern Anatolia (Fig. 1). The volcanic centers Ağrı, Nemrut, Süphan, and Tendürek are the most famous and form significant peaks, reaching an elevation of 5500 m at Ağrı These dormant/active volcanoes represent a significant threat to the surrounding populations. The reactivation and/or partial collapse of such a volcano in Eastern Anatolia could result in catastrophic consequences given the dearth of previous studies, hazard maps, emergency information programs, monitoring, and land-use planning. The Süphan stratovolcano is one of the most important Quaternary volcanic centers in the region. It is situated along the northern shore of Lake Van (Fig. 1) which extends for 130 km WSW-ENE and is the fourth largest lake in the world by volume (volume 607 km^3, area 3574 km^2, maximum depth 450 m) (Degens et al. 1984; Litt et al. 2009; Cukur et al. 2014). The Lake Van basin has formed in a tectonically active region (Şengör et al. 2003; Pınar et al. 2007). The northern and western parts of Lake Van are influenced by Pliocene and Quaternary volcanic eruptions (e.g., Nemrut and Süphan volcanoes; Karaoğlu et al. 2005; Özdemir et al. 2006, 2011; Özvan et al. 2015). Reactivation of any one of these volcanoes could cause tsunamis by entrance into the water of large pyroclastic flows or debris avalanches from edifice collapse. The results of this would be most devastating for the settlements of Van, Tatvan, Adilcevaz, and Ahlat (Fig. 1) around Lake Van.

Süphan volcano is formed by lava flows, lava domes, pyroclastic fall deposits, debris avalanches, and maar—related pyroclastic falls and flows (Figs. 1 and 2). Recent studies (Özdemir et al. 2012; Özdemir and Güleç 2014) suggest there was a debris avalanche in the volcanic past of Süphan, which travelled approximately 25 km north of the volcano. There has been no hazard assessment regarding the potential volcanic risk of Süphan volcano. The aim of this study is to characterize the Süphan Debris avalanche deposits, to make inferences regarding pre-avalanche topography and volume of the sector collapse, and to present a quantitative hazard assessment that includes future sector collapses and subsequent tsunamis using the numerical code *VolcFlow* (Kelfoun and Druitt 2005; Kelfoun et al. 2010).

Background geology

Süphan (lat. 38.550 N, long. 42.590 E) is a steep-sided stratovolcano that reaches ~4050 m above sea level, towering above the surrounding plains at 1700 m. It is located close to the northern coast of Lake Van. The volcanic center is located at the intersection of two major fault zones, trending NE–SW and NW–SE (Yılmaz et al. 1998). It has a base diameter of 40 km. Volcanic products of Süphan span an area of 2000 km^2 (Özdemir et al. 2011; Özdemir and Güleç 2014) and are emplaced over the Miocene and Pliocene-Pleistocene sedimentary units in eastern Anatolia (Fig. 2). The current morphology of Süphan is a complex volcano that resulted from the formation of a crater, domes, lavas, and pyroclastic fallout and flow deposits. It consists of a 2-km crater with a large, ellipsoidal, young summit dome (~64 ka) of 1 km in diameter and remnants rhyolitic domes. Beside the central edifice, several volcanic structures, including maars and domes, are present around the volcano. Detailed geological and petrological evolution of the Süphan stratovolcano is given in Özdemir et al. (2011) and Özdemir and Güleç (2014). The available radiometric ages range between 0.76 and 0.06 Ma (Özdemir and Güleç 2014). Observed initial products of Süphan volcanism include pyroclastic deposits, rhyolitic and perlitic lava flows, and associated debris avalanche deposits. These units are overlain by basaltic, basaltic trachyandesitic, and trachandesitic lava flows. Several plinian eruptions and a block and ash flow unit overlay these basic and intermediate units. Trachytic lava flows and rhyolitic/dacitic domes occurred during the last eruption phase of the main cone (Fig. 2). The most recent products of volcanism are phreatomagmatic and include the formation of a maar in the southern region of the volcano (Özdemir and Güleç 2014). The recent study of Schmincke et al. (2014) proposed the existence of younger Süphan tephra layers within the Lake Van sediments with an age range between 13,078 and 12,740 BP. These explosive products possibly originated from Aygır maar (Lake Aygır in Fig. 2), which is one of the youngest volcanic structure of the Süphan volcanic complex.

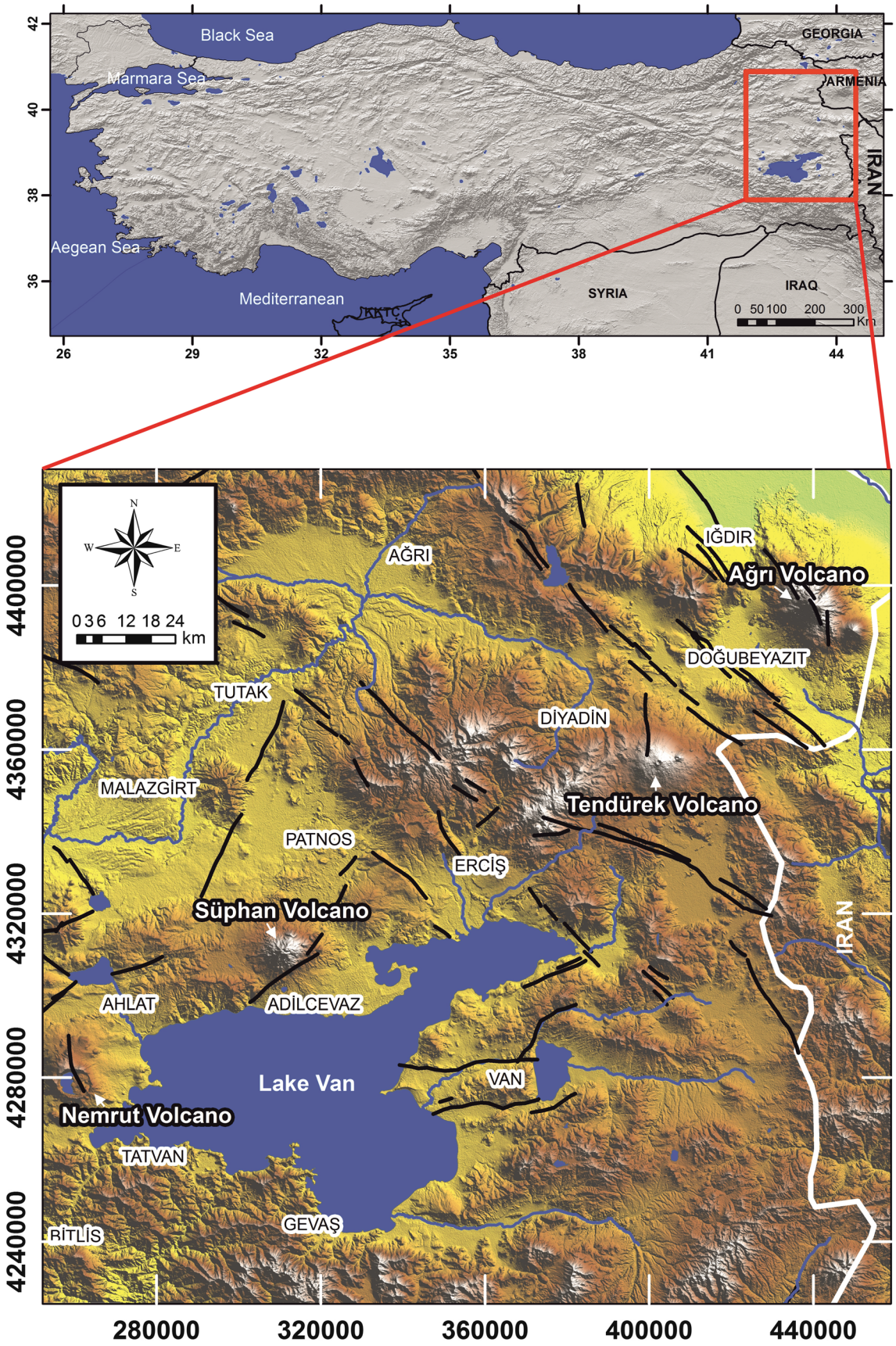

Fig. 1 Location of Süphan and some of the other Quaternary volcanoes (Ağrı, Nemrut and Tendürek) of the Eastern Anatolia, Turkey, and major towns and faults (*black lines*). Geographical coordinates are expressed in UTM projection, zone 38 S

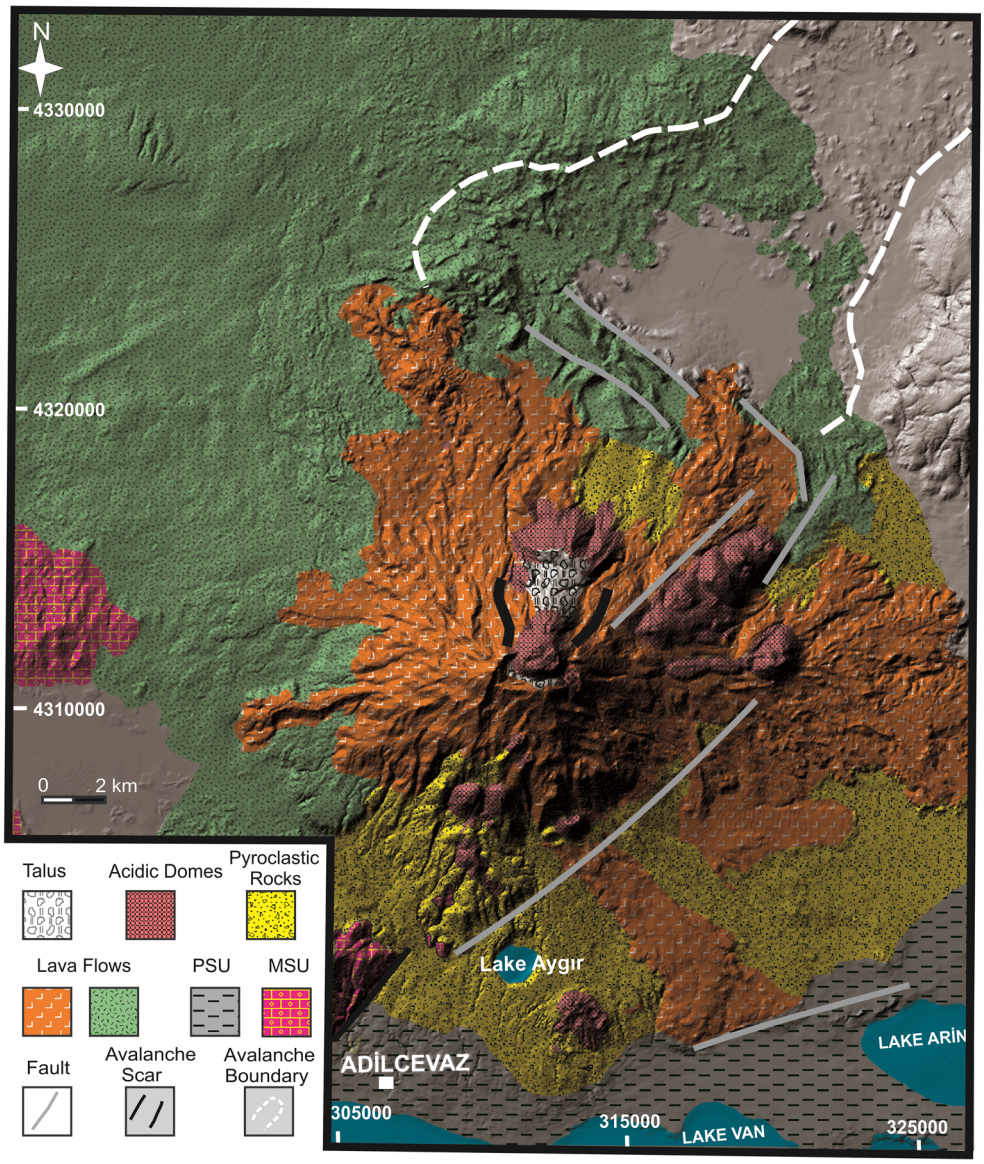

Fig. 2 Geological map of Süphan volcano (modified from Özdemir and Güleç 2014). *Green* represents mostly basaltic and basaltic trachyandesitic lava flows. *Orange* represents mostly trachyandesitic and trachytic lava flows. Lava flow ages 760 ± 40–150 ± 40 ka. Ages of dacitic domes 110 ± 30–64 ± 14 ka. Geographical coordinates are expressed in UTM projection, zone 38 S. *PSU* Pliocene sedimentary units, *MSU* Miocene sedimentary units

Süphan debris avalanche

A partial volcanic edifice collapse commonly generates a volcanic debris avalanche. A debris avalanche is a sudden, rapid flowage of wet or dry, incoherent, unsorted mixtures of rock, and matrix in response to gravity (Schuster and Crandell 1984).

The deposit is characterized by two depositional facies, "block" and "matrix" (Ui 1989; Sigurdsson et al. 2000). A debris avalanche block is a fractured and deformed piece of the source volcano included within a debris avalanche deposit. The sizes of single blocks vary from more than several hundred meters across to less than a meter. A debris avalanche matrix is a mixture of smaller volcanic clasts derived from various parts of the source volcano that forms the bulk of the deposit and often support the debris avalanche blocks. This facies is massive, poorly sorted, and made up of fragments of volcanoclastic formations and occasionally of fragments of paleosols and plants (Sigurdsson et al. 2000). An amphitheater-shaped scar is often observed at the source, and hummocky topography on the surface of the deposit is characteristic topographic features of a debris avalanche. Hummocky topography is composed of numerous hills and longitudinal and transverse ridges (Glicken 1982, 1996; Siebert 1984).

The Süphan debris avalanche deposit, which will be referred to as the SP-DAD, can be traced approximately 25 km to the north of the Süphan volcanic edifice. The most characteristic feature of SP-DAD is the hummocky topography, characterized by block facies and displaying ellipsoidal-circular hills and longitudinal-transverse ridges (Figs. 3 and 4a, b). The size of the hummocks decreases away from the source. Debris avalanche blocks are composed of rhyolite obsidian and perlite fragments (Fig. 4c). Sizes of the blocks

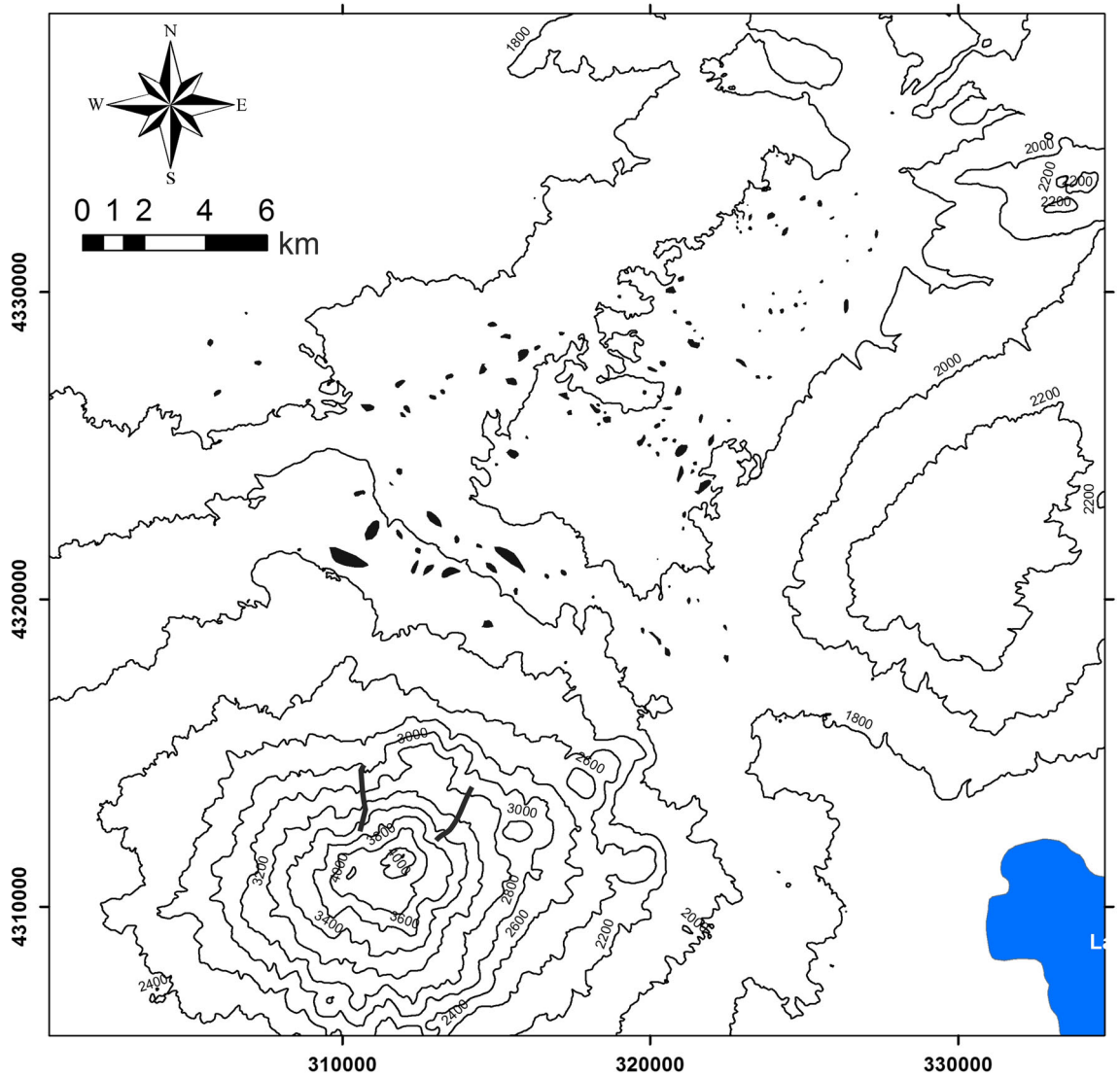

Fig. 3 Distribution of debris avalanche hummocks at northeast of Süphan volcano. *Solid lines* represent the avalanche scar. Contour interval is 200 m. Geographical coordinates are expressed in UTM projection, zone 38 S

reach up to 1.5–2 m in some outcrops, and most are angular. The size and the number of the large blocks decrease with increasing distance from the source. Siebert (1984) ascribed such decreasing size of the blocks in debris avalanche deposits as a result of progressive fracturing of megablocks as they move down the valley. Matrix facies of SP-DAD (Fig. 4d) consists of a mixture of rhyolitic obsidian, perlite, and some exotic material such as clay, fluvial gravel, and basement rocks. Exotic materials are eroded and mixed with the debris avalanche matrix material during flow. Matrix facies display gray, yellow, and brown colors and are mostly characterized by flat topography.

In the Süphan stratovolcano, the source area of the debris avalanche is obscured by later volcanic units and post avalanche erosion, and hence, the avalanche scar is not so visible on the volcanic edifice (Fig. 2). This makes it difficult to speculate on the possible triggering mechanisms for the debris avalanche. In the Süphan volcanic complex, dacitic and rhyolitic domes are present at the summit and on the flanks of the volcano. The ages of these domes are ranged between 110 ± 30 and 64 ± 14 ka. The youngest one is rhyolitic and has developed on the summit crater of the volcano and possibly plugs the main conduit of Süphan volcano. Additionally, some remnant older domes are present in the northern and eastern parts of the crater; however, the ages of these structures are not known. There are no syn-eruptive pyroclastic deposits associated with the debris avalanche deposits in the area. It is therefore difficult to suggest volcanic activity as the trigger with the available data. However, given the important role of tectonic structures in the evolution of the Süphan volcanism and the development of dacitic and rhyolitic domes

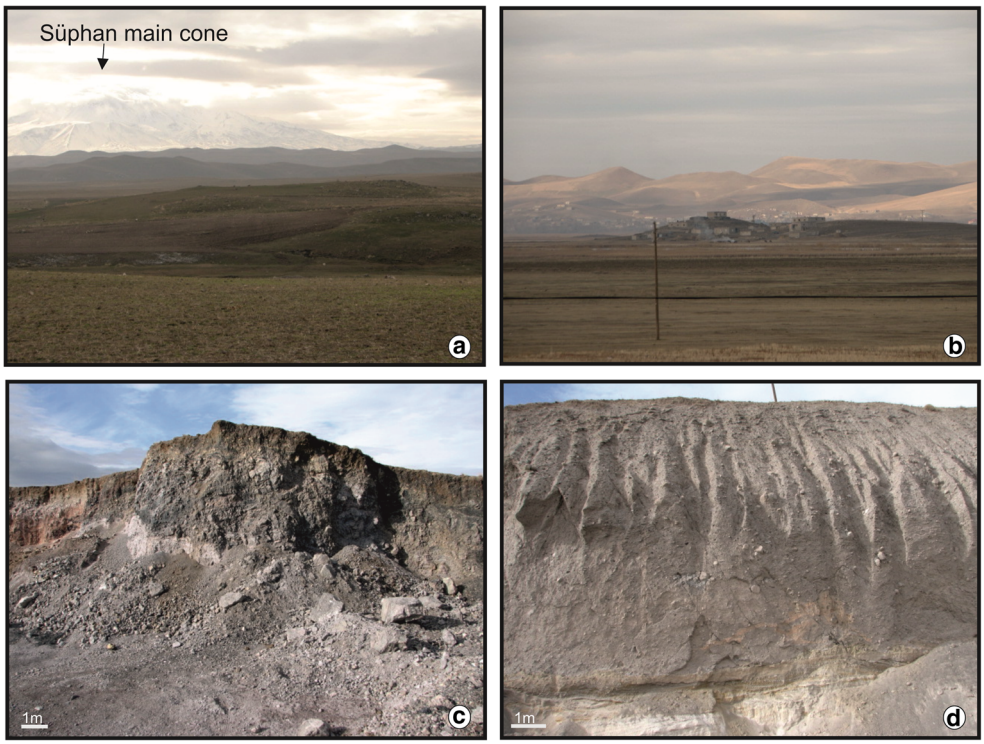

Fig. 4 Süphan debris avalanche hummocky topography seen from the northeast (**a**) and east (**b**). **c** Block facies (~15 km northeast of the main edifice) and **d** matrix (~20 km north of main edifice) of the SP-DAD

on the flanks and summit of the volcano, it is possible that a combination of magmatic and tectonic processes may be responsible for the sector collapse of Süphan.

Volume and age of the SP-DAD

The SP-DAD covers a large area of about 200 km^2 on the northern flanks of the Süphan volcano, reaching a distance of approximately 25 km. The dispersal area, the distal and marginal parts of the SP-DAD, are not well constrained due to the younger units of the Süphan volcanism. Mafic lava flows with low viscosity, and intermediate to acidic lavas of the Süphan have covered the SP-DAD. The observable thickness of the SP-DAD varies between 5 and 30 m, with an overall average estimated at 20 m. The estimated volume of the SP-DAD using the identified areal extent is 4 km^3. This estimated volume is not well constrained because part of the deposited has been eroded or buried under the younger units of the Süphan volcano. The age of the SP-DAD is also unknown, but the oldest Süphan volcanic unit that appear to overly the SP-DAD have been dated at 428 ± 40 ka (Özdemir et al. 2011; Özdemir and Güleç 2014) suggesting the SP-DAD is older. Most of the avalanche blocks in SP-DAD are a composition of obsidian and perlite. The study of Ogata et al. (1989) reported the K-Ar age of the Süphan obsidians as 760 ± 40 ka; if this age is true, the collapse of the Süphan northern flanks is possibly constrained between 428 and 760 ka.

Numerical model

Numerical simulations of debris and rock avalanches are being increasingly used for hazard assessment on volcanoes and will be essential for future hazard mitigation (e.g., Hungr and Evans 1996, 2004; Chen and Lee 2000; Crosta et al. 2004, 2009; McDougall and Hungr 2004; Pitman et al. 2003; Kelfoun and Druitt 2005). Among them, two rheological behaviors have been widely used to determine the basal shear stress for non-volcanic events, including the frictional (Savage and Hutter 1989) and Voellmy (Chen and Lee 2003) resistance equation. The first is exhibited by dry granular materials, in a wide range of shear rates and stresses. The second empirically accounts for rate-dependent resistance that may be due to the change of material behavior at high shearing strain rates or, possibly, to pore-fluid effects (Sosio and Crosta 2009). However, only a few volcanic debris avalanches (e.g., St. Helens, Socompa, Montserrat, Mt. Pelée, Soufrière Hills, Little Tahoma Peak, and Nevado de Toluca) have been numerically modeled to date. These examples have been best replicated by using a Coulomb frictional rheology (Le Friant et al. 2003; Heinrich et al. 2001; Sheridan et al. 2005; Capra et al. 2008), or a plastic rheology (Kelfoun and Druitt 2005).

The numerical code used for SP-DAD simulations is called VolcFlow (Kelfoun and Druitt 2005). This code specifically aims to simulate volcanic flows (pyroclastic flow, debris avalanche, lava flow). Sedimentation, erosion, and other geophysical flows, such as mud flow or tsunami, can also be simulated using VolcFlow (Kelfoun et al. 2010; Bernard

et al. 2014). The code is based on a depth-averaged approximation, where equations are solved using a shock-capturing numerical method based on a double upwind Eulerian scheme. The code is based on the assumption that the bulk of the avalanche slid on a thin basal layer (a common assumption for granular flow). The depth-averaged equations are solved on a topography-linked coordinate system with x and y as horizontal points (parallel to the local ground surface). After each time increment, new thicknesses and x and y components of the velocities are calculated.

For the simulation of tsunamis generated by debris avalanche, VolcFlow can simulate both the avalanche and the water together with their interactions. We use the same model as developed in Kelfoun et al. 2010: the tsunami is formed (1) by the topographic change cause by the avalanche through a pseudo 3D interaction and (2) by the drag between the avalanche and the water, which depends on the surface of the landslide in contact with the water and on the square of the relative velocity, following the work of Tinti et al. (2006). The depth-averaged approach is adapted for the simulation of flows whose extent is larger than their thickness. The debris avalanche as well as the depth/extent of the Lake Van is fully compatible with this approach. The variables used in our simulations are given in Table 1.

Reconstructed pre-edifice topography

Before using a numerical model for hazard assessment, it is important to check its quality by reproducing a past event, and this requires an accurate reconstruction of the topography. At Süphan volcano, an accurate reconstruction of the pre-avalanche topography is not possible because SP-DAD is one of the oldest units of the volcanism. The edifice collapse scarp that produced the SP-DAD was filled with post-collapse lava flows and rhyolitic domes. Thus, details of the deposits (morphology, thickness) such as those available for the Socompa volcano and its DAD (Kelfoun and Druitt 2005) cannot be used to validate or model. However, it is possible to reconstruct first-order morphology of the edifice to determine the best rheological parameters that allow the simulation of the thickness and the runout of the SP-DAD. Pre-collapse topography of SP-DAD and the surrounding valley was reconstructed from the 25-m interval contours of the 1/25.000 topographic map. Debris avalanche deposits and post avalanche volcanic units are removed to gain the paleotopography of the terrain on which the SP-DAD flowed. It is probable that the pre-collapse height of Süphan was lower than the current elevation and also that the topography of the summit could mostly differ from the current topography. A very approximate estimate of the volume of the collapse material can be made by subtracting the pre-collapse topography from the post-collapse topography. The is estimated volume is about 1.75 km^3; adding the expansion of 25–30 % (Voight et al. 1983) of material during the avalanche gives a volume of ~2.2 km^3. Only the visible hummocks at the northern parts of the volcano are used for this estimation. Some of the hummock-like structures that were completely covered by post-avalanched younger lavas were not taking into account during the calculation. This explains why the derived value of 2.2 km^3 is quite different from the estimated volume of 4 km^3 calculated using the dispersal area and average thickness.

Digital elevation models (DEMs) with a 25-m spatial resolution are derived for the reconstructed pre-collapse topography without SP-DAD and post avalanche deposits by interpolating between edited contours, using the Triangular Irregular Network method (TIN). The DEM of the pre-collapse topography is used as an input file of the VolcFlow model, together with a set of parameters to model the ancient sector collapse of Süphan volcano and to find the best fit parameters to model a future edifice collapse scenario of the current volcanic edifice. The parameters used in modeling are as follows: ρ, the avalanche density; φ_{int}, internal angle of friction; φ_{bed}, basal angle of friction; and additional friction coefficients that can be constant or can depend (linearly or to the second power) upon debris avalanche velocity. This enables the modeling of frictional (with one or two friction angles), viscous, Bingham, Voellmy, or other avalanche flow behaviors (Kelfoun and Druitt 2005). The SP-DAD is modeled using different rheological laws and a range of parameters. Flow density was kept constant as 2000 kg/m^3. Different volumes of the collapse scar are used during the simulations to obtain the best fit with the SP-DAD by means of matching the flow run out and deposit distribution, as well as some morphological features.

The frictional avalanche rheology was first tested using three possible combinations, as in Kelfoun and Druitt

Table 1 Main variables used in simulations

Variable	Value	Unit
Gravity	9.78	m s^{-2}
Time	100–200–400	s
Flow density	2000	kg m^{-3}
Water density	1000[b]	kg m^{-3}
Viscosity	0.001	Pa s
Volume of flows	2 to 6	km^3
Internal angle of friction (φ_{int})	0[a]	degrees
Basal angle of friction (φ_{bed})	2[a]	degrees
Constant retarding stress	50	kPa
Mean velocity	~55[b]	m s^{-1}
Cs	0.01[b]	–
Cf	2[b]	–

"Flow" refers to the avalanching material

[a] Frictional avalanche models

[b] Tsunami model

(2005), (1) $\varphi_{bed} << \varphi_{int} = 30°$; (2) $\varphi_{bed} \neq 0°$ *but* $\varphi_{int} = 0°$; (3) $\varphi_{int} = \varphi_{bed} \neq 0°$. In each case, the parameters were varied in multiple simulations. Most of the scenarios do not tend to simulate SP-DAD accurately. In general, taking the collapse scar volume constant (3 km^3), high frictional coefficients (φ_{bed} and φ_{int}) reduce the run out distance of SP-DAD. For our initial best fit model (Fig. 5a–d), $\varphi_{int} = 0$ and a value of $\varphi_{bed} = 2$ is required to reach the northeastern edge of the deposit. However, eastern and northwestern lateral distributions are not very realistic. Based on the best available field data, the products of SP-DAD were not observed at the eastern and northwestern parts of the volcano, as in Fig. 5. However, the thickness of proximal deposits is not similar to the observed SP-DAD. Increasing the basal and internal friction angles decreases the run out distance and increases the lateral spreading.

The second best fit is obtained using a constant retarding stress in the range of 50–100 kPa (Dade and

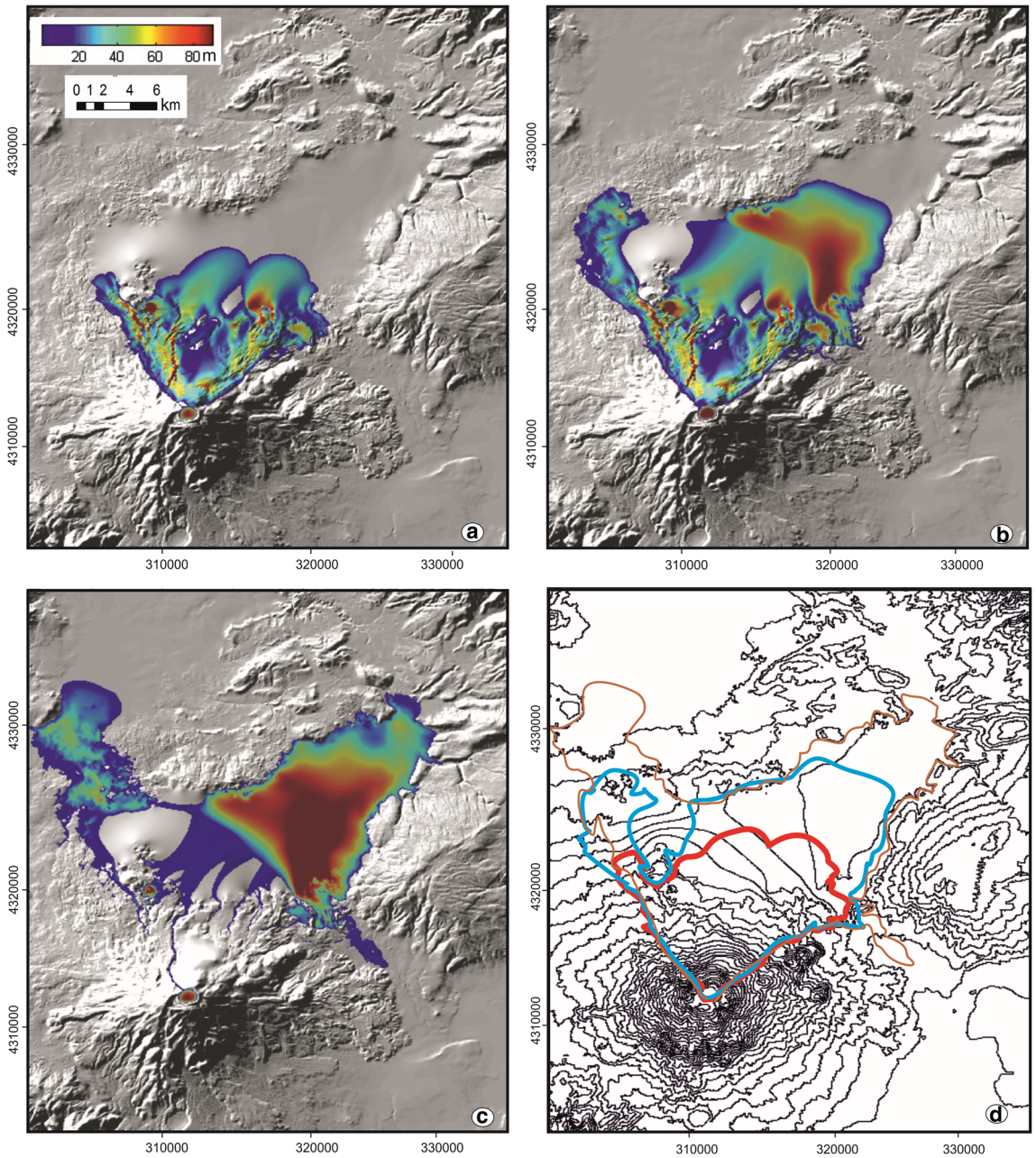

Fig. 5 Snapshots of the emplacement of frictional avalanche models with a volume of 3 km^3 at $t = 100$ s, $t = 200$ s and until the rest of avalanche (400 s), with the corresponding deposits. **a–c** Avalanche simulated with φint = 0 φbed = 2. The *color scale* denotes the thicknesses (m) of the avalanche. **d** Outlines of the final deposits. *Red*, $t = 100$ s; *Blue*, $t = 200$ s; *Brown*, $t = 400$ s. Geographical coordinates are expressed in UTM projection, zone 38 S

Huppert 1998). Kelfoun and Druitt (2005) also argued that unlike the frictional rheologies, this constant retarding stress law produces a deposit with a well-defined edge and levées with a deposit of realistic thickness on all slopes, irrespective of slope angle. Using a different collapse scar volume (1–4 km^3) and constant retarding stress in the range of 50–100 kPa, the models provide a good fit. Using a volume of 4 km^3 for collapse scar and with a constant retarding stress of 50 kPa (Fig. 6a–d), northeastern run out distance and eastern lateral distribution of SP-DAD are reproduced. However, the western distribution of the model is much greater than the observed deposit distribution.

The estimated approximate volume of the SP-DAD is 4 km^3, a similar collapse volume fit with the run out distance and some lateral distribution of the SP-DAD. However, if the erosional, buried part of the debris avalanche deposit is taken into account the volume of the SP-DAD should be somewhat higher than this approximation.

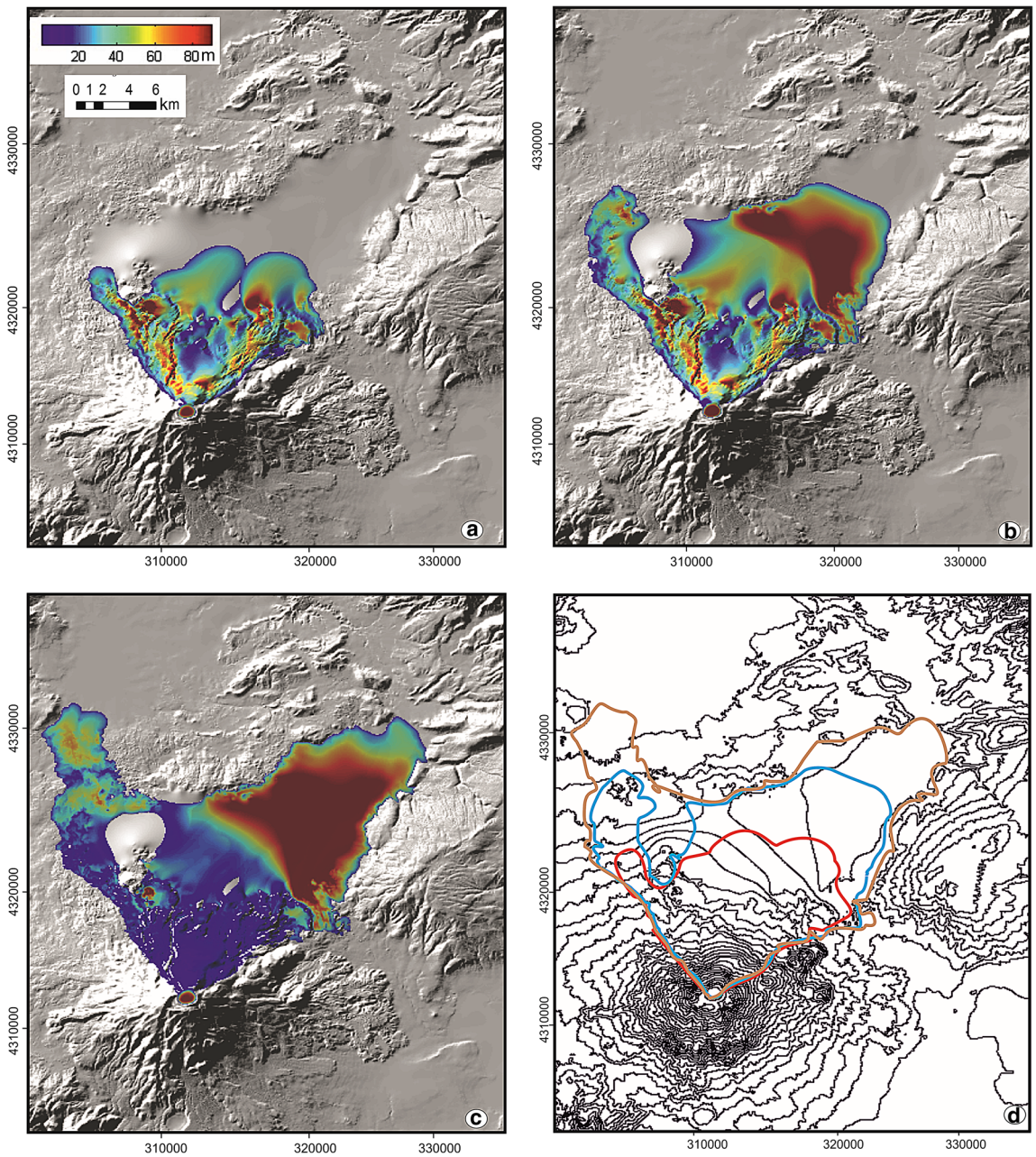

Fig. 6 Avalanche evolution using a constant retarding stress $T = 50$ kPa and a volume of 4 km^3. The *color scale* denotes thickness. **a**–**c** Snapshots at 100, 200, and 400 s. **d** Outlines of the final deposits. *Red*, $t = 100$ s; *Blue*, $t = 200$ s; *Brown*, $t = 400$ s. Geographical coordinates are expressed in UTM projection, zone 38 S

Possible hazard scenarios

One of the main hazardous events of Süphan, judging from its deposits, is debris avalanche. Süphan volcano has various domes on the summit crater. These domes together with lava flows have filled the avalanche scar. In this study, we simulate two scenarios mainly based on the collapse of these structures: (1) collapse of the new edifice northward from Süphan volcano, and (2) a southward edifice collapse. The northern-collapse scenario would be similar to the emplacement of the SP-DAD previously discussed. In the case of the southern scenario, a debris avalanche would enter Lake Van and trigger a tsunami.

Vulnerability of the region

The vulnerability of an area to natural processes results from the combined spatial distributions of natural processes and human activity (demography, economy) (Pouget et al. 2012). The economy of an entire region around Süphan volcano relies on agriculture and livestock. Many inhabitants live under the risk of an edifice collapse from the Süphan volcano.

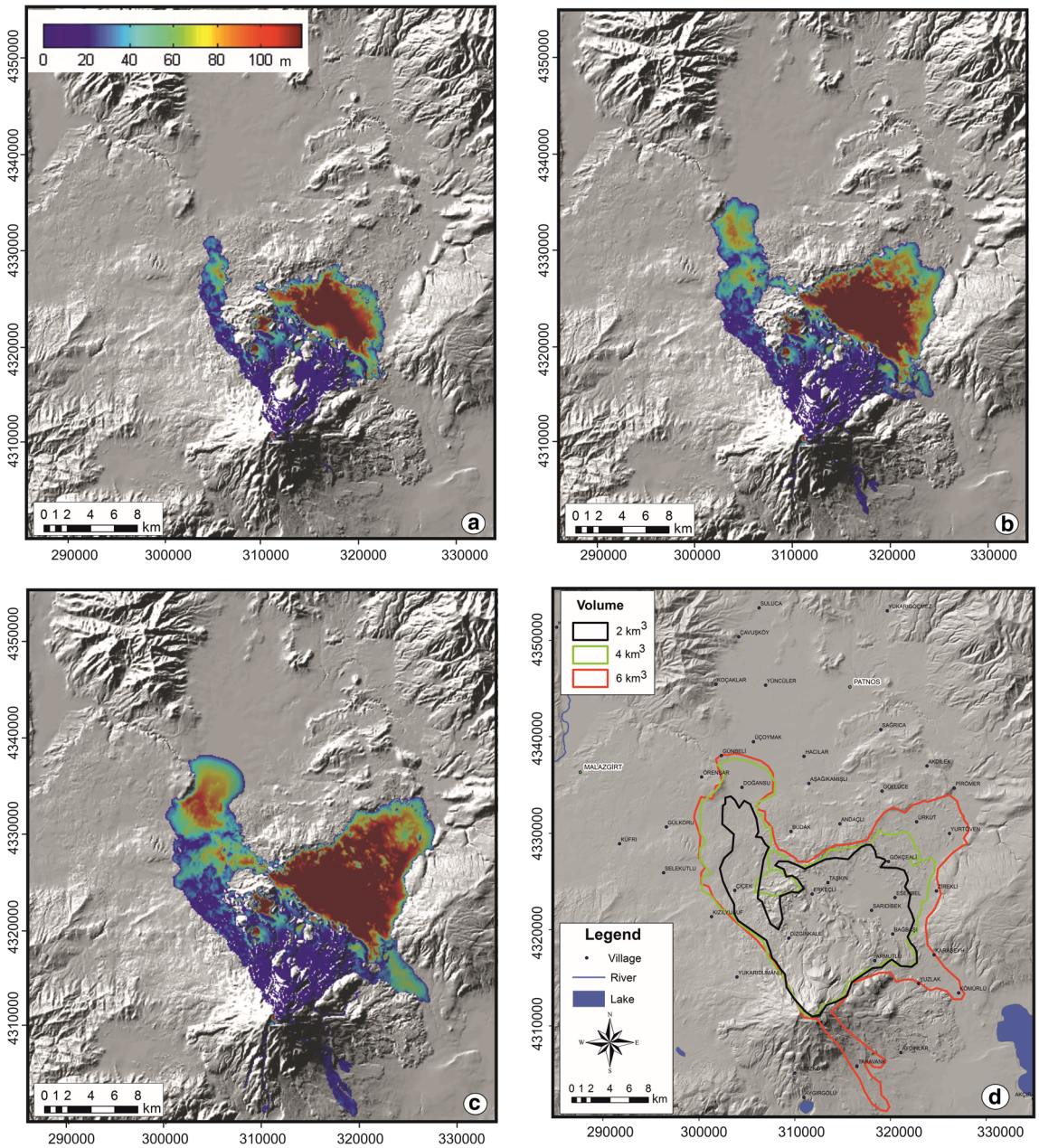

Fig. 7 Avalanche evolution using a constant retarding stress $T = 50$ kPa. The *color scale* denotes thickness. **a**–**c** Snapshots at 400 s for a volume of 2,4, and 6 km^3, respectively. **d** Avalanche-related hazard map exposed towns of the northern region of Süphan volcanic complex. Geographical coordinates are expressed in UTM projection, zone 38 S

However, in the case of emplacement of a debris avalanche into Lake Van, the number of people at risk is increased due to the additional threat of an avalanche-triggered tsunami.

Northward edifice collapse scenario

To conduct a hazard assessment for emplacement of a debris avalanche, the recent topography of Süphan volcano was constructed from the 25-m interval contours of the 1/25.000 topographic map. The first (northern) scenario models are run with a constant retarding stress of 50 kPa, which gave the best fit for modeling the previous debris avalanche of Süphan. Several models are run with a constant retarding stress of 50 kPa and density of 2000 kg/m^3. In each model, only the volume of the collapse scar is changed, and the models are run for $t = 100$ s, 200 s, and for the duration of the avalanche (400 s). In Fig. 7, volume for 2, 4, and 6 km^3 debris avalanches at $t = 400$ s are shown. The edge thickness of deposits is different for each volume. These thicknesses range between 20, 25, and 35 m for 2, 4, and 6 km^3, respectively. The hummocks, lateral levees, and transverse ridges of the older debris avalanche, as well as the younger domes and lava ridges of the Süphan Volcanic Complex, behave like barriers and prevent the flow from reaching higher run out distances. With a collapse scar volume of 6 km^3, the products of the modeled debris avalanche can reach the vicinity of Malazgirt, one of the biggest towns of the region. The hazard map of the SPDAD for different volumes is shown in Fig. 7e.

Southward edifice collapse scenario and tsunami

In this study, we simulate several tsunami scenarios originating from different volumes of flank collapses of the Süphan Volcano towards the South. For this purpose, we combine our digital elevation model (DEM) with Lake Van bathymetry data (the bathymetry data is from "Lake Van Drilling Project-PaleoVan", Litt et al. 2009; Cukur et al. 2014). Again, we use the numerical code *VolcFlow* (Kelfoun and Druitt 2005; Kelfoun et al. 2010; Giachetti et al. 2011) to simulate both Süphan debris avalanche and the tsunami propagations with different collapse volumes (2, 3, 4, 5, and 10 km^3) to determine the magnitude of wave arrival and to characterize the dynamics of the tsunami.

In all scenarios, coastal settlements are affected by the tsunamis. The simulated debris avalanches spread south of the volcano and then enter the lake, pushing and lifting the water surface tens of meters above the initial level. Tsunami run-ups range from 6 to 10 m on the shoreline of Lake Van (Fig. 8)

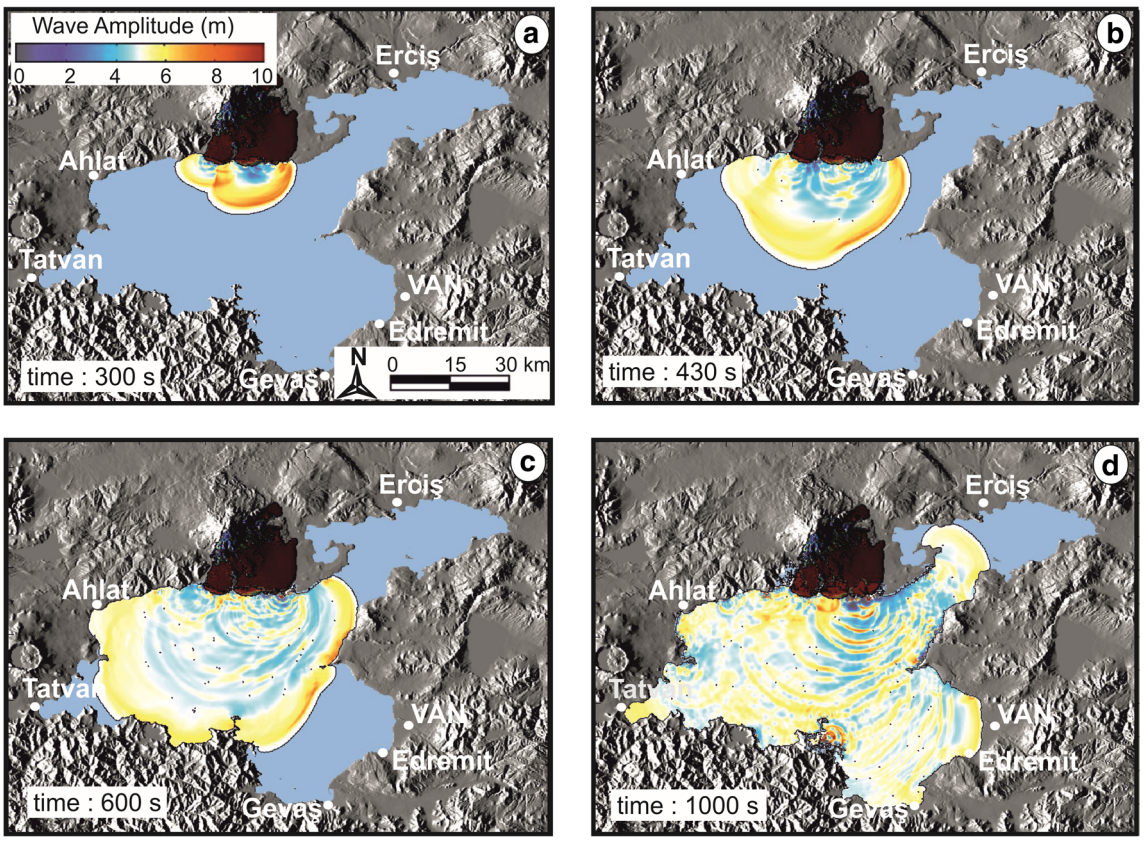

Fig. 8 Water amplitude (meters) generated by a volume of 4 km^3 avalanche at **a** $t = 300$ s (4.06 min), **b** 430 s (6.54 min), **c** 600 s (8.27 min), and **d** 1000 s (14.02 min). Debris avalanche deposits appear as *dark shading*

producing wave amplitudes that could exceed 10 m at land fall. The avalanche reaches a maximum distance of ~25 km to the southeast at a mean velocity of ~55 m s^{-1}. Numerical results presented here are calculated using a volume of 4 km^3, in a single-event collapse, avalanche/water interaction parameters values of $C_s = 0.01$ and $C_f = 2$ (Tinti et al. 2006; Kelfoun et al. 2010), and a constant retarding stress rheology of 50 kPa for the avalanche. Water density is 1000 kg m^{-3} with a viscosity of 0.001 Pa s. Figure 8 shows four propagation stages for the waves using a single-event collapse with a constant retarding stress of 50 kPa. Five minutes after the onset of the avalanche, the resulting waves reach 10 m (Fig. 8a). The first wave would reach the city of Van, approximately 14 min after the onset of the debris avalanche, with amplitude of nearly 8 m. This would be followed by another ~6 m wave, with a smaller period of 17 min after the onset of the avalanche (Fig. 8d). Subsequently, there would be several smaller and shorter waves. Adilcevaz and Ahlat, which are located to the southwest, are one of the first towns affected by the tsunami, after 4 and 7 min, respectively (Fig. 8b). Tatvan, the second largest settlement, is affected by the tsunami after 12 min (Fig. 8c). Gevaş and Edremit, which are located on the southern shoreline of Lake Van, are affected by the tsunami after 12.5 min (Fig. 8d). The northeastern coast is protected by the shape of the lake and is affected by waves less than 5 m in amplitude (Fig. 8d).

Conclusions

Eastern Anatolian Quaternary volcanoes have often been considered as inactive. However, recent studies suggest the presence of relatively young volcanic products (e.g., Schmincke et al. 2014) and an active magma chamber at mid crustal depths between Nemrut and Süphan volcanoes (e.g., Angus et al. 2006). These dormant/active volcanoes represent a significant threat to the surrounding populations. This study is the first to provide a quantitative hazard assessment for Süphan Volcano by modeling the emplacement of debris avalanches and an associated tsunami that would result from different partial edifice collapse scenarios. The SP-DAD covers a large area of northern flanks of the Süphan volcano, reaching a distance of over 25 km with dispersal area of roughly 200 km^2. We have simulated the older Süphan debris avalanche by using various parameters to obtain a best fit by means of matching with known flow run out and deposit distribution, as well as some morphological features. The best fit is obtained for a 4-km^3 failure volume, which is similar to the volume of SP-DAD estimated from its thickness and areal distribution. A large number of people could be threatened by the consequences of another edifice collapse from Süphan. In the case of a southward edifice collapse, the debris avalanche would enter into Lake Van, thus greatly increasing the number of people threatened by an associated tsunami.

Acknowledgments The constructive reviews of Nilgün Güleç, R.A. Brooker, and JC Komorowski and editors Jacopo Taddeucci and James D.L. White considerably improved the manuscript and are gratefully acknowledged.

References

Angus DA, Wilson DC, Sandvol E, Ni JF (2006) Lithospheric structure of the Arabian and Eurasian collision zone in eastern Turkey from S-wave receiver functions. Geophys J Int 166:1335–1346

Bernard J, Kelfoun K, Le Pennec JL, Vargas SV (2014) Pyroclastic flow erosion and bulking processes: comparing field-based vs. modeling results at Tungurahua volcano, Ecuador. Bull Volcanol 76:1–16

Borselli L, Capra L, Sarocchi D, De la Cruz-Reyna S (2011) Flank col-406 lapse scenarios at volcan de Colima, Mexico: a relative instability analysis. J Volcanol Geotherm Res 208:51–65

Capra L, Norini G, Groppelli G, Macías JL, Arce JL (2008) Volcanic hazard zonation of Nevado de Toluca volcano. J Volcanol Geotherm Res 176:469–484

Chen H, Lee CF (2000) Numerical simulation of debris flows. Can Geotech J 37(1):146–160

Chen H, Lee CF (2003) A dynamic model for rainfall-induced landslides on natural slopes. Geomorphology 51:269–288

Crosta GB, Chen H, Lee CF (2004) Replay of the 1987 Val Pola landslide, Italian alps. Geomorphology 60(1–2):127–146

Crosta GB, Imposimato S, Roddeman D (2009) Numerical modelling of entrainment/ deposition in rock and debris-avalanches. Eng Geol 109(1–2):135–145

Cukur D, Krastel S, Schmincke HU, Sumita M, Çağatay MN, Meydan AF, Damcı E, Stockhecke M (2014) Seismic stratigraphy of lake Van, eastern Turkey. Quat Sci Rev 104:63–84

Dade WB, Huppert HE (1998) Long-runout rockfalls. Geology 26:803–806

Degens ET, Wong HK, Kempe S, Kurtmann F (1984) A geological study of Lake Van, eastern Turkey. Geol Rundsch 73(2):701–734

Devoli G, Cepeda J, Kerle N (2009) The 1998 casita volcano flank failure revisited—new insights into geological setting and failure mechanisms. Eng Geol 105:65–83

Giachetti T, Paris R, Kelfoun K, José Pérez-Torrado F (2011) Numerical modelling of the tsunami triggered by the Güimar debris avalanche, Tenerife (Canary Islands): comparison with field-based data. Mar Geol 284:189–202

Glicken H (1982) Criteria for identification of large volcanic debris avalanches (abstr). EOS Trans Am Geophys Union 63:1141

Glicken H (1986) Rockslide–debris avalanche of May 18, 1980, Mount St. Helens volcano. PhD dissertation, Univ Santa Barbara, 303 pp

Glicken H (1996) Rockslide-debris avalanche of the May 18, 1980, Mount St. Helens Volcano, Washington, U.S. Geol. Surv. Open-file Rep., 96–677

Heinrich P, Boudon G, Komorowski JC, Sparks RSJ, Herd R, Voight B (2001) Numerical simulation of the December 1997 debris avalanche in Montserrat. Geophys Res Lett 28(13):2529–2532

Hungr O, Evans SG (1996) Rock avalanche runout prediction using a dynamic model, Proc. 7th Int. Symp. on Landslides. Int Symp on Landslides 1:233–238

Hungr O, Evans SG (2004) Entrainment of debris in rock avalanches: an analysis of a long run-out mechanism. Geol Soc Am Bull 116:1240–1252

Karaoğlu Ö, Özdemir Y, Tolluoğlu AÜ, Karabıyıkoğlu M, Köse O, Froger JL (2005) Stratigraphy of the volcanic products around

Nemrut Caldera: implications for reconstruction of the caldera formation. Turk J Earth Sci 14:123–143
Keating BH, McGuire WJ (2000) Island edifice failures and associated tsunami hazards. Pure Appl Geophys 157:899–955
Kelfoun K, Druitt TH (2005) Numerical modeling of the emplacement of Socompa rock avalanche, Chile. J Geophys Res 110, B12202
Kelfoun K, Giachetti T, Labazuy P (2010) Landslide-generated tsunamis at Réunion Island. J Geophys Res 115, F04012. doi:10.1029/2009JF001381
Kerle N, van Wyk de Vries B (2001) The 1998 debris avalanche at Casita volcano, Nicaragua: investigation of structural deformation as the cause of slope instability using remote sensing. J Volcanol Geotherm Res 105(1–2):49–63
Kerle N, van Wyk de Vries B, Oppenheimer C (2003a) New insight into the factors leading to the 1998 flank collapse and lahar disaster at Casita volcano, Nicaragua. Bull Volcanol 65:331–345
Kerle N, Froger J-L, Oppenheimer C, van Wyk de Vries B (2003b) Remote sensing of the mudflow at Casita volcano, Nicaragua. Int J Remote Sens 24(23):4791–4816
Le Friant A, Heinrich P, Deplus C, Boudon G (2003) Numerical simulation of the last flank- collapse event of Montagne Pelee, Martinique, lesser Antilles. Geophys Res Lett 30(2):1034
Litt T, Krastel S, Sturm M, Kipfer R, Örcen S, Heumann G, Franz SO, Ülgen UB, Niessen F (2009) 'PALEOVAN', international continental scientific drilling program (ICDP): site survey results and perspectives. Quat Sci Rev 28:1555–1567
Mc Guire W (1996) Volcano instability: a review of contemporary themes. Geol Soc Lond Spec Publ 110:1–23
McDougall S, Hungr H (2004) A model for the analysis of rapid landslide motion across three-dimensional terrain. Can Geotech J 41:1084–1097
Ogata A, Nakamura K, Nagao K, Akimoto S (1989) K-Ar age of young volcanic rocks of Turkey. Annual meeting of the Geochemical Society of Japan, ICO 3
Özdemir Y, Güleç N (2014) Geological and geochemical evolution of the quaternary Süphan stratovolcano, eastern Anatolia, Turkey: evidence for the lithosphere-asthenosphere interaction in post-collisional volcanism. J Petrol 55:37–62
Özdemir Y, Karaoğlu Ö, Tolluoğlu AÜ, Guleç N (2006) Volcanostratigraphy and petrogenesis of the Nemrutstratovolcano (East Anatolian Plateau): the most recent post-collisional volcanism in Turkey. Chem Geol 226:189–211
Özdemir Y, Blundy JD, Güleç N (2011) The importance of fractional crystallization and magma mixing in controlling chemical differentiation at Süphan stratovolcano, eastern Anatolia, Turkey. Contrib Mineral Petrol 162:573–597
Özdemir Y, Oyan V, Güleç N (2012) Süphan Volkanik Çığı'nın Jeolojik Özellikleri Yüzüncü Yıl Üniversitesi Fen Bilimleri Enstitüsü Dergisi. J Ins Nat App Scie 17(1):1–5
Özvan A, Dinçer İ, Akın M, Oyan V, Tapan M (2015) Experimental studies on ignimbrite and the effect of lichens and capillarity on the deterioration of Seljuk Gravestones. Eng Geol 185:81–95
Pınar A, Honkura Y, Kuge K, Matsushima M, Sezgin N, Yilmazer M, Öğütçü Z (2007) Source mechanism of the 2000 November 15 Lake Van earthquake (Mw = 5.6) in eastern Turkey and its seismotectonic implications. Geophys J Int 170(2):749–763
Pitman EB, Patra AK, Bauer A, Sheridan MF, Bursik MI (2003) Computing debris flows and landslides. Phys Fluids 15:3638–3646
Pouget S, Davies T, Kennedy B, Kelfoun K, Leyrit H (2012) Numerical modelling: a useful tool to simulate collapsing volcanoes. Geol Today 28:59–63
Savage SB, Hutter K (1989) The motion of a finite mass of granular material down a rough incline. J Fluid Mech 199:177–215
Schmincke HU, Sumita M, Paleovan scientific team (2014) Impact of volcanism on the evolution of Lake Van (eastern Anatolia) III: periodic (Nemrut) vs. episodic (Süphan) explosive eruptions and climate forcing reflected in a tephra gap between ca. 14 ka and ca. 30 ka. J Volcanol Geotherm Res 285:195–213
Schuster RL, Crandell DR (1984) Catastrophic debris avalanches from volcanoes. Proc. IV hit. Symp. on landslide. Toronto 1:567–572
Scott KM, Macías JL, Naranjo JA, Rodríguez S, McGeehin JP (2001) Catastrophic debris flows transformed from landslides in volcanic terrains: mobility, hazard, assessment, and mitigation strategies. U.S. Geological Survey Professional Paper 1630
Scott KM, Vallance JW, Kerle N, Macías JL, Strauch W, Devoli G (2005) Catastrophic precipitation-triggered lahar at casita volcano, Nicaragua: occurrence, bulking and transformation. Earth Surf 30:59–79
Şengör AMC, Özeren S, Zor E, Genc T (2003) East Anatolian high plateau as a mantle supported, N-S shortened modal structure. Geophys Res Lett 30(24):8045. doi:10.1029/2003GL017858
Sheridan MF, Stinton AJ, Patra A, Pitman EB, Bauer A, Nichita CC (2005) Evaluating Titan 2D mass-flow model using the 1963 little Tahoma peak avalanches, Mount Rainier, Washington. J Volcanol Geotherm Res 139(1–2):89–102
Siebert L (1984) Large volcanic debris avalanches: characteristics of source areas, deposits, and associated eruptions. J Volcanol Geotherm Res 22:163–197
Siebert L (2002) Landslides resulting from structural failure of volcanoes. In: Evans SG, DeGraff JV (eds) Catastrophic landslides: effect, occurrence, and mechanisms. Geological Society of America Reviews in Engineering Geology, Boulder XV, pp 209–235
Siebert L, Glicken H, Ui T (1987) Volcanic hazards from Bezymianny- and Bandai-type eruptions. Bull Volcanol 49:435–459
Sigurdsson H, Houghton B, McNutt SR et al (eds) (2000) Encyclopedia of volcanoes. CA, Academic Press, San Diego
Sosio R, Crosta GB (2009) Rheology of concentrated granular suspensions and possible implications for debris flow modeling. Water Resour Res 45(W03412):16
Sosio R, Crosta GB, Hungr O (2011) Numerical modeling of debris avalanche propagation from collapse of volcanic edifices. Landslides 9:315–334
Stoopes GR, Sheridan MF (1992) Giant debris avalanches from the Colima volcanic complex, Mexico: implications for long-runout landslides (>100 km) and hazard assessment. Geology 20:299–302
Tinti S, Pagnoni G, Zaniboni F (2006) The landslides and tsunamis of the 30th of December 2002 in Stromboli analysed through numerical simulations. Bull Volcanol 68:462–479
Ui T (1983) Volcanic dry avalanche deposits-identification and comparison with non-volcanic debris stream deposits. In: Aramaki S, Kushiro I (eds). Arc Volcanism. Journal Volcanol Geotherm Res 18: 135–150
Ui T (1989) Discrimination between debris avalanches and other volcaniclastic deposits. In: Latter, J.H. (Ed.), Volcanic Hazards. IAVCEI Proc. in Volcanology. Springer-Verlag, Heidelberg, 1: pp. 201–209
Ui T, Takarada T and Yoshimoto M (2000) Debris avalanches, Encyclopedia of Volcanoes, H. Sigurdsson, ed., Academic Press, San Diego, California, pp. 617–626
van Wyk de Vries B, Kerle N, Petley D (2000) A sector collapse forming at Casita volcano, Nicaragua. Geology 28:167–170
Voight B, Glicken H, Janda RJ, Douglass PM (1981) Catastrophic rockslide avalanche of May 18. In: Lipman P W, Mullineaux D R (eds) The 1980 eruptions of Mount St. Helens, Washington. U S Geol Surv Prof Pap 1250:347–348
Voight B, Janda RJ, Glicken H, Douglass PM (1983) Nature and mechanics of the Mount St. Helens rockslide-avalanche of 18 May 1980. Geotechnique 33(3):243–273
Yılmaz Y, Güner Y, Şaroğlu F (1998) Geology of the quaternary volcanic centers of the east Anatolia. J Volcanol Geotherm Res 85:173–210